AIAA JOURNAL
Vol. 46, No. 12, December 2008

Separated-Shear-Layer Development on an Airfoil at Low Reynolds Numbers

Serhiy Yarusevych*
University of Waterloo, Waterloo, Ontario N2L 3G1, Canada
John G. Kawall†
Ryerson University, Toronto, Ontario M5B 2K3, Canada
and
Pierre E. Sullivan‡
University of Toronto, Toronto, Ontario M5S 3G8, Canada

DOI: 10.2514/1.36620

Flow transition in the separated shear layer on the upper surface of a NACA 0025 airfoil at low Reynolds numbers was investigated. The study involved wind-tunnel experiments and linear stability analysis. Detailed measurements were conducted for Reynolds numbers of 100,000 and 150,000 at 0-, 5- and 10-degree angles of attack. For all cases examined, laminar boundary-layer separation takes place on the upper surface of the airfoil. The separated shear layer fails to reattach to the airfoil surface for the lower Reynolds number, but reattachment occurs for the higher Reynolds number. Despite this difference in flow development, experimental results show that a similar transition mechanism is attendant for both Reynolds number flow regimes. Flow transition occurs due to the amplification of natural disturbances in the separated shear layer within a band of frequencies centered at some fundamental frequency. The initial growth of disturbances centered at the fundamental frequency is followed by the growth of a subharmonic component, eventually leading to flow transition. The growing disturbances also cause shear-layer roll-up and the formation of roll-up vortices. The results show that inviscid stability theory can be employed to adequately estimate such salient characteristics as the frequency of the most amplified disturbances and their propagation speed. This implies that the roll-up vortices can be attributed to inviscid instability. However, the results suggest that viscous and nonparallel effects need to be accounted for to effectively model the convective growth of the disturbances in the separated shear layer.

Nomenclature

c	=	airfoil chord
c_r	=	propagation speed of the disturbances, $2\pi f/\alpha_r$
E_{uu}	=	normalized energy spectrum of u
f	=	frequency
f_0	=	fundamental frequency of the disturbances
Re_c	=	Reynolds number, $U_0 c/\nu$
U	=	x components of local instantaneous velocity
$\bar{U}$	=	time average of U
U_0	=	freestream velocity in the x direction
u, v	=	x and y fluctuating velocity components
u'_f	=	root-mean-square value of bandpass-filtered u
$\hat{v}$	=	amplitude function of disturbances imposed on v
x, y	=	streamwise and vertical coordinates
α	=	angle of attack
α^*	=	complex wave number, $\alpha_r + i\alpha_i$
α_r	=	wave number
$-\alpha_i$	=	growth rate
λ	=	streamwise distance between roll-up vortices
ν	=	kinematic viscosity of air
ω	=	circular frequency of disturbances, $2\pi f$

Received 11 January 2008; accepted for publication 3 August 2008.

*Assistant Professor, Department of Mechanical and Mechatronics Engineering, 200 University Avenue West. Member AIAA.
†Associate Professor, Department of Mechanical and Industrial Engineering, 350 Victoria Street.
‡Associate Professor, Department of Mechanical and Industrial Engineering, 5 King's College Road. Member AIAA.

I. Introduction

THE flowfield around an airfoil operating at low Reynolds numbers Re_c differs significantly from classical aeronautical applications. In particular, at chord Reynolds numbers below about 500,000, a laminar boundary layer on the upper surface of the airfoil often separates, forming a separated shear layer (e.g., [1,2]). Lifting surfaces operate at low Reynolds numbers in many engineering applications, including micro air vehicles and wind turbines. Previous experimental results discussed by Mueller and DeLaurier [2] indicate that below Reynolds numbers of about 50,000, the separated shear layer does not reattach to the airfoil surface. At higher Reynolds numbers, the separated shear layer may reattach to the airfoil surface, resulting in a laminar separation bubble. In both cases, laminar boundary-layer separation has a significant detrimental effect on airfoil performance, adversely effecting airfoil lift and drag. The behavior of the separated shear layer and the extent of the separation region are major factors that determine the severity of this effect. Therefore, accurate evaluation of the characteristics and the extent of the separated-flow region is crucial for designing effective airfoils and assessing airfoil performance.

A key feature of airfoil boundary-layer development at low Reynolds numbers is the laminar-to-turbulent transition in the separated shear layer. This transition has a profound effect on the characteristics of the separated-flow region and can lead to shear-layer reattachment. Following the pioneering work of Gaster [3] and Horton [4], most of the previous studies that focused on separated-shear-layer development were performed for a separation bubble forming on a flat plate in an adverse pressure gradient rather than on an airfoil surface [5–12]. Nevertheless, they provide valuable insight into the transition process. In particular, it has been demonstrated that small-amplitude fluctuations in the attached boundary layer, originating from freestream disturbances through the receptivity process, are significantly amplified beyond the separation point (e.g., [5,6]). The initial stage of the transition process is associated with the

exponential growth of the disturbances centered at some fundamental frequency [6,7]. It has been shown in both experimental and numerical investigations [8–11] that two-dimensional instabilities experience the highest growth at this stage. The last stage of transition, which results in rapid flow breakdown to turbulence, is three-dimensional in nature and is associated with nonlinear interactions between the two-dimensional instabilities (e.g., [11]).

Also, in a number of studies, coherent structures that form during transition have been shown to play a dominant role in separation-bubble formation [5,10,11]. Experimental results obtained by Watmuff [5] revealed the cat's-eye pattern associated with the Kelvin–Helmholtz instability in phase-averaged spanwise vorticity contours. These structures were shown to become three-dimensional further downstream and to persist into the attached turbulent boundary layer. Studies by Lang et al. [10] and Marxen and Rist [11] revealed vortices in the separated shear layer that form due to the roll-up of the shear layer. Although the downstream evolution of these structures was not investigated in detail, the results suggest a rapid breakdown of the roll-up vortices in the reattachment region.

A number of studies have been performed on various airfoil profiles to study boundary-layer separation and separated-shear-layer development at low Reynolds numbers (e.g., [13–24]). However, compared with investigations on a flat plate in an adverse pressure gradient, there are fewer studies focused on the transition process in the airfoil's separated shear layer. The available results show some trends similar to those observed on a flat-plate geometry. In particular, a number of experimental investigations suggest that the initial stage of transition is associated with the exponential growth of two-dimensional disturbances in the separated shear layer (e.g., [18–20]). This is followed by nonlinear interactions between the disturbances, and three-dimensional breakdown results.

In a numerical study, Lin and Pauley [21] showed that coherent structures form within a separation bubble on an airfoil and persist downstream of the reattachment. The authors argued that these structures are attributed to the Kelvin–Helmholtz instability (cf., [5]). The experimental results of Burgmann et al. [22] indicate the formation of roll-up vortices in a separation bubble on an airfoil. However, the downstream development of these structures was found to be different from that observed on a flat plate by Watmuff [5] and Lang et al. [10], suggesting that the surface curvature may affect the development of the separated shear layer. There are also a limited number of studies that complemented experimental data with stability calculations. For the boundary-layer separation on a flat plate at an angle of attack, Nishioka et al. [23] demonstrated that inviscid stability calculations are in reasonable agreement with experimental data. LeBlanc et al. [24], in what appears to be a rare example involving experiments on an airfoil, applied linear stability theory to predict the frequency of the most amplified disturbance in the separated shear layer and the growth rate of the disturbances. Their numerical results show reasonable agreement with experimental data; however, calculations were based on Falkner–Skan profiles, similar to experimental mean velocity profiles.

It should be noted that the aforementioned studies were performed for the case when a separation bubble forms on an airfoil surface, whereas the development of a separated shear layer without reattachment has not been addressed. Preliminary stability calculations presented by Yarusevych et al. [20] showed reasonable agreement with experimental data and serve as a motivation for the present work.

The present study is aimed at gaining added insight into the development of a separated shear layer on an airfoil operating in low Reynolds number flows by combining experimental and analytical approaches. In particular, it is of interest to study the evolution of flow disturbances and their role in the transition process in the separated shear layer for the cases when laminar separation occurs without reattachment and when a separation bubble is formed on an airfoil surface.

II. Experimental Setup

Experimental investigations were performed in a low-turbulence recirculating wind tunnel. The 5-m-long test section of this tunnel has a spanwise extent of 0.91 m and a height of 1.22 m (Fig. 1). One of the side walls of the test section is made of Plexiglas for operational and visualization purposes. The background turbulence intensity level in the test section is less than 0.1%. During the experiments, the freestream velocity was monitored by a pitot tube, with an uncertainty estimated to be less than 2.5%.

A symmetrical NACA 0025 aluminum airfoil with a chord length c of 0.3 m was examined. This profile was selected because it allowed investigating both strongly separated flows and separation bubbles at relatively low angles of attack and the Reynolds numbers of interest. The airfoil was mounted horizontally in the test section (Fig. 1), spanning the entire width of the test section. Mean-flow uniformity over at least 50% of the airfoil span was verified experimentally [25]. The origin of the streamwise coordinate x was located at the leading edge of the airfoil, and the vertical coordinate y was referenced to the airfoil surface. Investigations were conducted for three angles of attack ($\alpha = 0$, 5, and 10 deg) and three Reynolds numbers ($Re_c = 55 \times 10^3$, 100×10^3, and 150×10^3). The angle of attack was set by a digital protractor, with an uncertainty of 0.1%.

Velocity data were obtained with a constant-temperature anemometer. A normal hot-wire probe was used. All hot-wire measurements were carried out in the vertical midspan plane of the tunnel. The probe was mounted on a remotely controlled traversing gear, which allowed probe motion in the vertical y and streamwise x directions with a resolution of 0.01 and 0.25 mm, respectively. The probe holder was mounted on a streamlined sting, and the angle between the probe and the airfoil surface could be manually adjusted. Following the recommendations of Brendel and Mueller [19], this angle was kept below 7 deg $\pm$0.1 deg to ensure negligible probe interference. With this arrangement, it was verified experimentally that the probe had no appreciable effect on the upstream flow development for the cases examined herein.

Based on the results of Kawall et al. [26], the uncertainty of hot-wire measurements was estimated to be less than 5%. For spectral analysis of the velocity signals, the duration of a sampled signal segment was sufficiently large to provide a frequency-resolution bandwidth of 1.2 Hz, which is adequate for resolving narrow peaks in the velocity spectrum. Based on the number of averages involved in obtaining the velocity spectra, the uncertainty of the spectral analysis was estimated to be approximately 4.5%. To allow adequate comparison of the spectra [20], velocity data used for spectral analysis were acquired at y/c positions corresponding to $0.5U_0$ in the separated shear layer (matching the location of the maximum rms streamwise velocity), and all presented spectra were normalized by the variance of the sampled velocity signal. Spectral analysis of the freestream velocity signals established that there was no significant frequency-centered activity associated with the approach flow.

A smoke-wire technique was employed for flow visualization. Two smoke wires were installed in the test section: one 15 cm

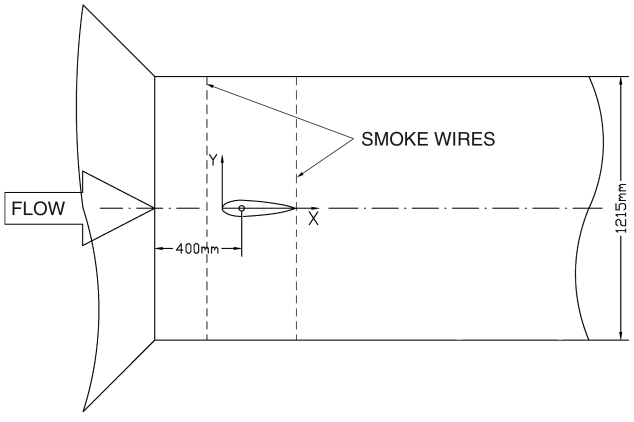

Fig. 1 Test section.

upstream of the airfoil leading edge and another immediately downstream of the trailing edge (Fig. 1). Each smoke wire was coated manually with smoke-generating fluid. The fluid was evaporated by means of resistive heating from a variable transformer, marking streaklines in the flow. A thin 0.076-mm-diam stainless steel wire was chosen to provide adequate smoke density while avoiding the introduction of measurable disturbances into the flowfield. The flow was illuminated with a remotely triggered speed light, and the flow-visualization images were acquired with a digital camera.

III. Results

Figure 1 shows flow-visualization results for three Reynolds numbers: $Re_c = 55 \times 10^3$, 100×10^3, and 150×10^3 at $\alpha = 5$ deg. The results reveal two distinct flow regimes: 1) boundary-layer separation without subsequent shear-layer reattachment for $Re_c = 55 \times 10^3$ and 100×10^3 (Figs. 2a and 2b) and 2) the formation of a separation bubble on the upper surface of the airfoil for $Re_c = 150 \times 10^3$ (Fig. 2c). In the case of $Re_c = 55 \times 10^3$ and 100×10^3, the boundary layer on the upper surface of the airfoil separates and a wide wake is formed.

Because of flow separation, the upstream smoke wire cannot be used to visualize flow inside a recirculation region, which forms past the separation point. Thus, the recirculation region is visualized by the smoke entrained in the upstream direction from the downstream smoke wire. In the case of $Re_c = 150 \times 10^3$, the flow is attached at the trailing edge of the airfoil and a closed recirculation region (i.e., a separation bubble) is formed at the mid chord. The observed boundary-layer behavior was verified by means of velocity measurements with a normal hot-wire probe.

A detailed examination of the flow-visualization results pertaining to $Re_c = 55 \times 10^3$ and 100×10^3 at $\alpha = 5$ deg (Figs. 2a and 2b) reveals organized structures forming in the separated shear layer on the upper surface ($x/c = 0.5$ to 0.75). For $Re_c = 150 \times 10^3$ (Fig. 2c), oscillations in the streakline adjacent to the separated-flow region on the upper surface at $x/c > 0.5$ also suggest the presence of organized structures in the separated shear layer. These structures can be investigated in more detail via the images of the separated region for $Re_c = 55 \times 10^3$ and 100×10^3, shown in Fig. 3. For both Reynolds numbers, there are several vortices generated in the separated shear layer on the upper surface. It is evident that the vortices form close to the interface between the recirculation region and the separated shear layer. These vortices likely originate from the roll-up of the separated shear layer and are similar in appearance to those observed in free shear layers.

As the Reynolds number increases to $Re_c = 100 \times 10^3$, the length scale of the roll-up vortices decreases substantially compared with the case of $Re_c = 55 \times 10^3$ and they do not propagate as far downstream as for the lower Reynolds number. The downstream spacing of the roll-up vortices is approximately constant in the corresponding images for $Re_c = 55 \times 10^3$ and 100×10^3, suggesting that for a given Reynolds number, the roll-up occurs at a constant frequency. The flow-visualization results demonstrate that the roll-up vortices eventually break down, and they suggest that the breakdown process is linked to the formation of a turbulent boundary layer, agreeing with recent findings of Burgmann et al. [22].

To gain further insight into the transition process, detailed hot-wire velocity measurements were performed for $Re_c = 100 \times 10^3$ and 150×10^3 at $\alpha = 0$, 5, and 10 deg. These two Reynolds numbers were chosen because they are associated with two distinctly different shear-layer developments at the three angles of attack investigated: viz., 1) separation without subsequent shear-layer reattachment ($Re_c = 100 \times 10^3$) and 2) the formation of a separation bubble ($Re_c = 150 \times 10^3$). For $Re_c = 100 \times 10^3$, laminar separation occurs on the upper surface of the airfoil at approximately $x/c = 0.35$, 0.3, and 0.18 for $\alpha = 0$, 5, and 10 deg, respectively [20]. For $Re_c = 150 \times 10^3$, a separation bubble forms on the airfoil surface at approximately $0.5 < x/c < 0.8$, $0.5 < x/c < 0.8$, and $0.34 < x/c < 0.54$ for $\alpha = 0$, 5, and 10 deg, respectively [20].

It should be noted that a single hot-wire probe is incapable of determining flow direction. Specifically, such a probe cannot resolve the velocity direction within the separated-flow region near the airfoil surface on which reverse flow occurs. Nevertheless, important information about boundary-layer separation can be extracted from the hot-wire measurements in the reverse flow region [19]. Hot-wire measurements in the separated shear layer, which is of particular interest, can be analyzed without any restrictions.

Spectra of the streamwise velocity component pertaining to the separated shear layer are presented in Fig. 4. The amplitude of each spectrum is increased by 1 order of magnitude with respect to that of the spectrum at the previous upstream location. The results reveal a similar transition mechanism for all cases examined.

Initially, no distinct frequency-centered activity is observed in the spectra pertaining to the laminar separated shear layer forming just downstream of the separation point. However, as the separated shear layer develops, disturbances within a specific frequency band are amplified. Within this band of frequencies, disturbances centered at a fundamental frequency f_0 experience the highest growth rate and

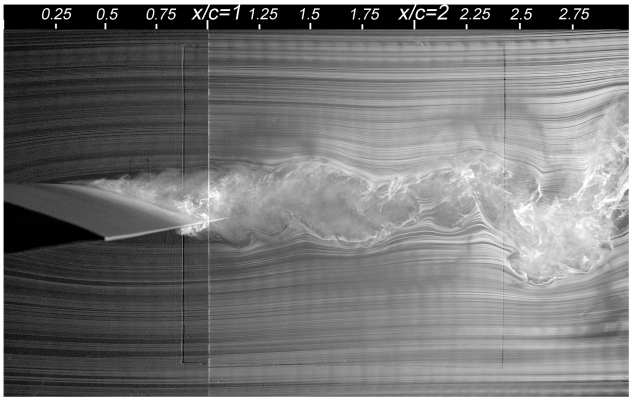

a) Re_c=55×10^3

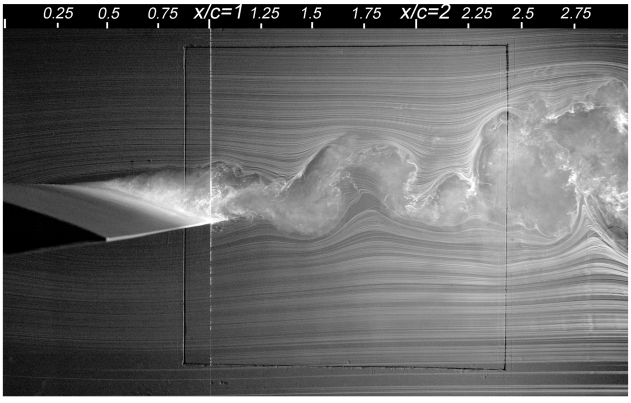

b) Re_c=100×10^3

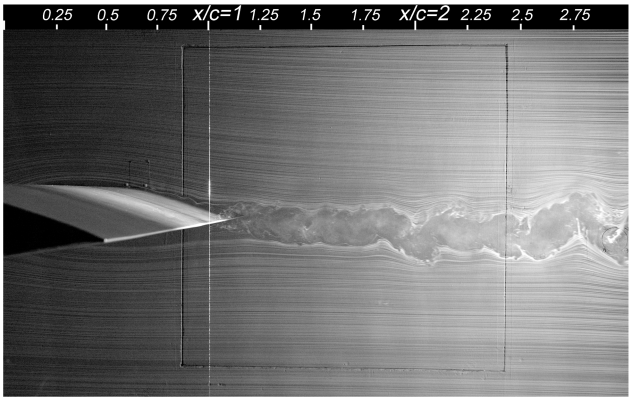

c) Re_c=150×10^3

Fig. 2 Smoke-wire flow visualization at $\alpha = 5$ deg.

persist further downstream, eventually leading to flow transition. For example, for $Re_c = 100 \times 10^3$ at $\alpha = 5$ deg (Fig. 4c), a flat spectrum typical of laminar shear flows is observed at $x/c = 0.37$.

As the separated shear layer develops downstream, a band of unstable Fourier components occurs centered at the fundamental frequency $f_0 = 165$ Hz ($x/c = 0.44$). Further downstream, nonlinear interactions between the disturbances take place, as evidenced by the growth of a subharmonic peak in the spectrum at $x/c = 0.53$ [7]. Eventually, this process leads to flow transition, with a typical turbulence spectrum observed at $x/c = 0.72$. It is of interest to compare these results (Fig. 4c) with the corresponding flow visualization (Fig. 3b). Clearly, the presence of roll-up vortices in the flow (Fig. 3b) should produce a peak in the spectrum of the velocity signal obtained at the corresponding location. Indeed, the dominant frequency-centered activity in the corresponding velocity spectra (Fig. 4c) occurs at the fundamental frequency. Thus, it can be concluded that the amplified disturbances cause the roll-up of the separated shear layer, leading to the formation of the roll-up vortices.

Although the initial roll-up occurs at the fundamental frequency, downstream development of the roll-up vortices occurs over the nonlinear growth region, and vortices eventually break down during the transition process. As the Reynolds number increases to $Re_c = 150 \times 10^3$ at $\alpha = 5$ deg, a similar transition mechanism is observed (Fig. 4d). However, the band of the amplified disturbances in the separated shear layer is centered at a higher value of $f_0 = 455$ Hz. As the separated shear layer develops downstream, disturbances in this frequency band are substantially amplified and, following a subharmonic growth, a spectrum typical of turbulent flow occurs at $x/c = 0.72$. It can also be inferred from the spectral results that the frequency band of the amplified disturbances broadens and the growth of the disturbance amplitude increases with the increase of the Reynolds number.

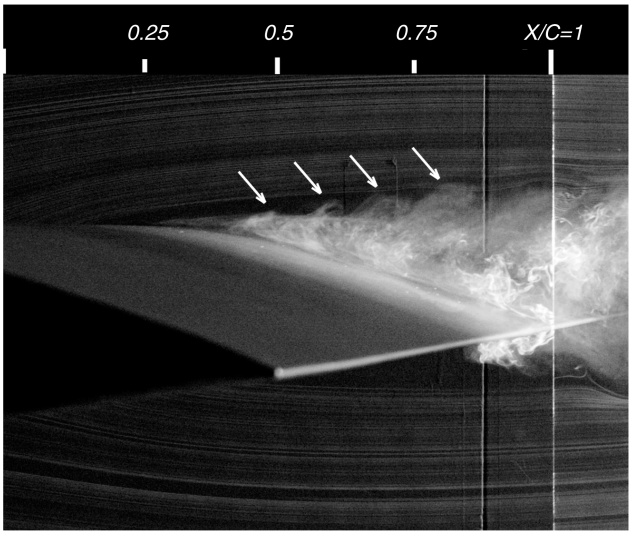

a) Re_c=55×10³

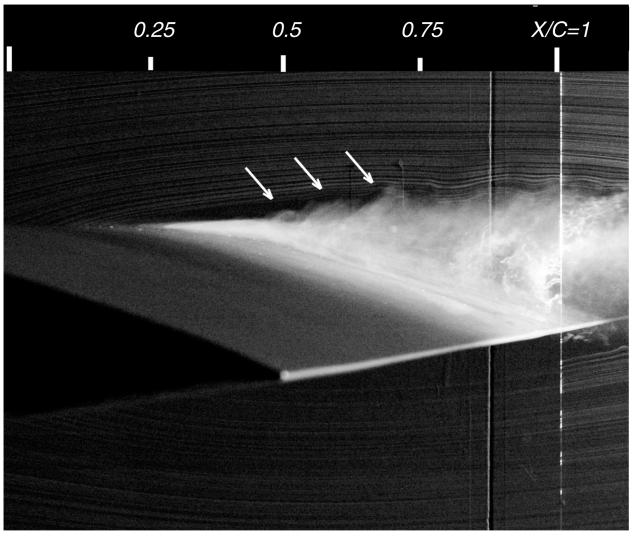

b) Re_c=100×10³

Fig. 3 Flow visualization of the separated layer at $\alpha = 5$ deg; shear-layer roll-up vortices are marked by arrows.

It is of interest to model the shear-layer transition process to gain better insight into the nature of the observed roll-up vortices, as well as to predict frequencies pertaining to the most amplified disturbances in the separated shear layer. Shear-layer stability analysis was carried out based on inviscid linear stability theory [27,28]. Following a detailed derivation from [27], the development of the inviscid disturbances can be described by the celebrated Rayleigh equation:

$$\hat{v}'' - \left(\frac{\alpha^* \bar{U}''}{\alpha^* \bar{U} - \omega} + \alpha^{*2} \right) \hat{v} = 0 \tag{1}$$

where the prime denotes differentiation with respect to y. In the present investigation, disturbances vanish at the wall and in the freestream; consequently,

$$\hat{v}(0) = \hat{v}(\infty) = 0 \tag{2}$$

Equations (1) and (2) govern the development of inviscid disturbances. Based on experimental results, it is appropriate to consider spatial growth of the disturbances. In this case, the disturbances are described by a real frequency ω and a complex wave number $\alpha^* = \alpha_r + i\alpha_i$. The real part α_r of this quantity is a wave number and the imaginary part α_i is a growth rate, which also identifies decaying ($\alpha_i > 0$) and growing ($\alpha_i < 0$) disturbances. Equation (1), with the boundary conditions given by Eq. (2), represents an eigenvalue problem that can be solved to yield a dispersion relation of the form

$$\alpha^* = \alpha^*(\omega) \tag{3}$$

The part of this dispersion relation that pertains to growing disturbances (i.e., $\alpha_i < 0$) is of particular interest. To obtain the dispersion relation, mean velocity profiles are required. The relevant mean velocity data obtained with a single hot-wire probe are presented in Fig. 5. As can be seen from the velocity spectra in Fig. 4, each data set in Fig. 5 corresponds to the portion of the separated shear layer at which disturbances experience the initial linear growth. In particular, nonlinear interactions, manifested by the subharmonic growth [7], are not present at the corresponding x/c locations and transition occurs further downstream.

Obviously, a conventional single hot-wire probe does not resolve the direction of the reverse flow that occurs near the airfoil surface in the separated-flow region. However, following the results of Watmuff [5] and Nishioka et al. [23], hot-wire velocity measurements obtained within the reverse flow in the laminar portion of a separated-flow region can be used to adequately estimate the magnitude of the mean streamwise velocity. Specifically, their results show that mean streamwise velocities of in the core of the reversed flow can be estimated from the corresponding measured velocities as $\bar{U} = -(\bar{U})_{\text{measured}}$. However, it has been shown by Durst and Zanoun [29] that in the immediate vicinity of the airfoil surface, the hot-wire measurements may be affected by additional heat losses, resulting in overestimated velocity readings. It was determined experimentally that for the cases investigated, the wall effect is confined to the region $0 < y/c < 0.002$. This is in agreement with the velocity data in Fig. 5, in which an erroneous increase of velocity is notable for $y/c < 0.002$. Thus, data points within the affected region must be discarded. On the other hand, because all of the profiles are within the laminar portion of the separated shear layer, mean streamwise velocities in the reverse flow region away from the wall ($y/c > 0.002$) can be estimated as $\bar{U} = -(\bar{U})_{\text{measured}}$ [5,23].

The obtained profiles are shown by solid lines in Fig. 5, which are plotted via a smoothing spline interpolation applied to the corrected

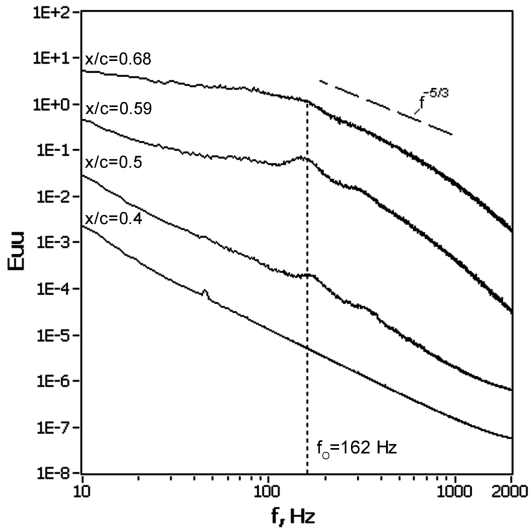

a) $Re_c=100\times10^3$, $\alpha=0°$

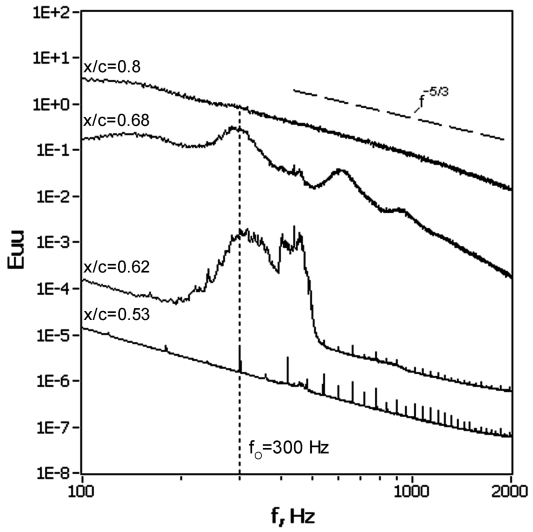

b) $Re_c=150\times10^3$, $\alpha=0°$

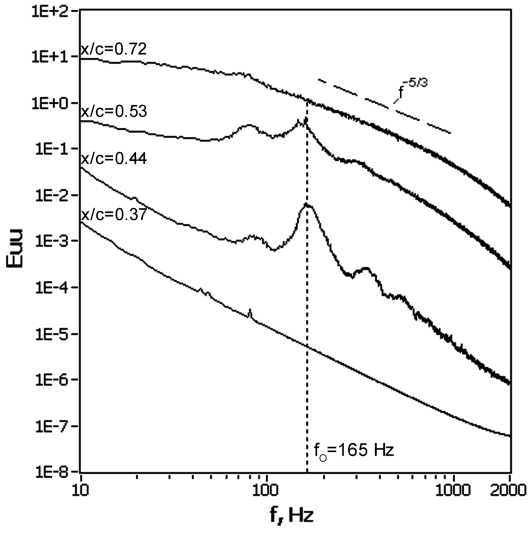

c) $Re_c=100\times10^3$, $\alpha=5°$

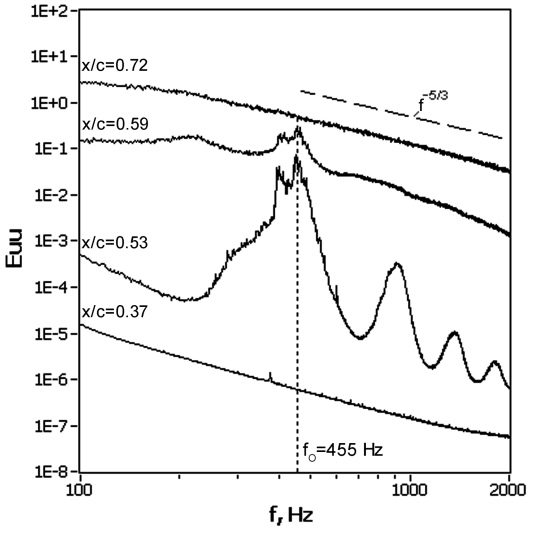

d) $Re_c=150\times10^3$, $\alpha=5°$

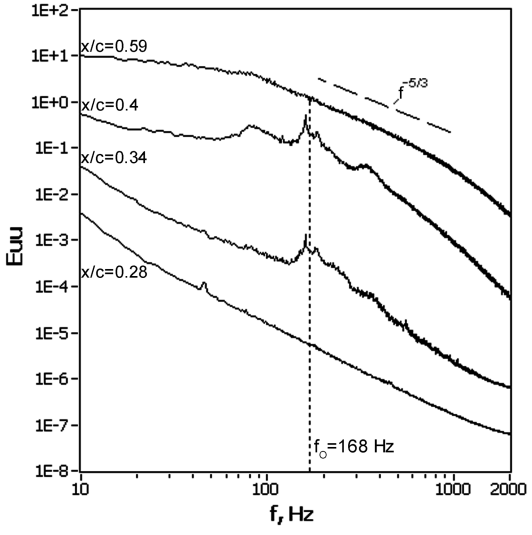

e) $Re_c=100\times10^3$, $\alpha=10°$

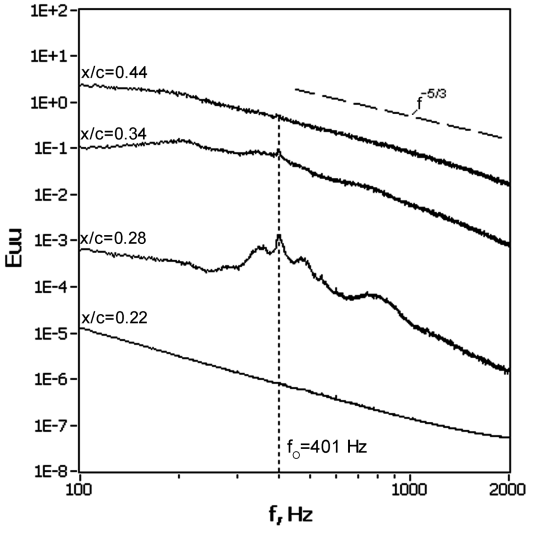

f) $Re_c=150\times10^3$, $\alpha=10°$

Fig. 4 Spectra of the streamwise fluctuating velocity component; for clarity, the amplitude of each successive spectrum is stepped by 1 order of magnitude.

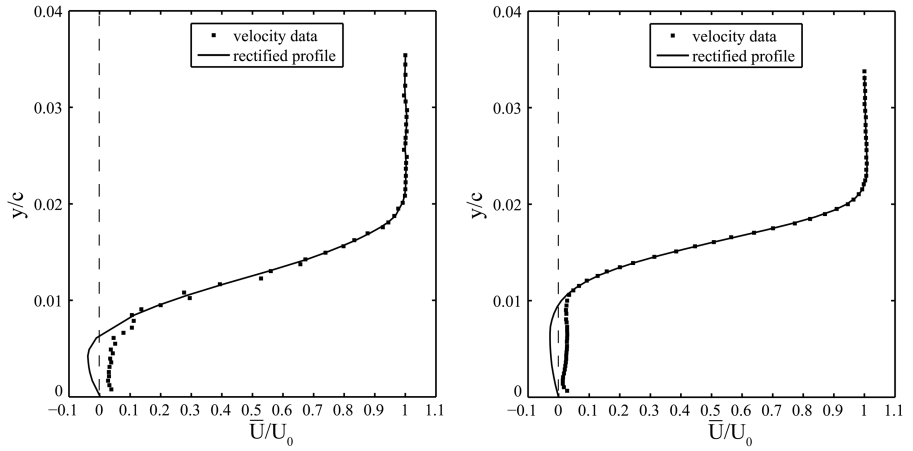

a) Re_c=100×10^3, α=0°, x/c=0.44

b) Re_c=150×10^3, α=0°, x/c=0.62

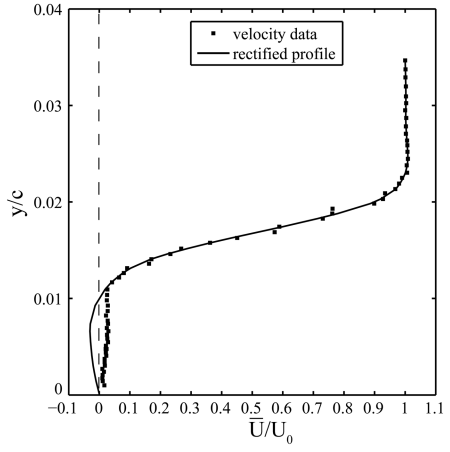

c) Re_c=100×10^3, α=5°, x/c=0.37

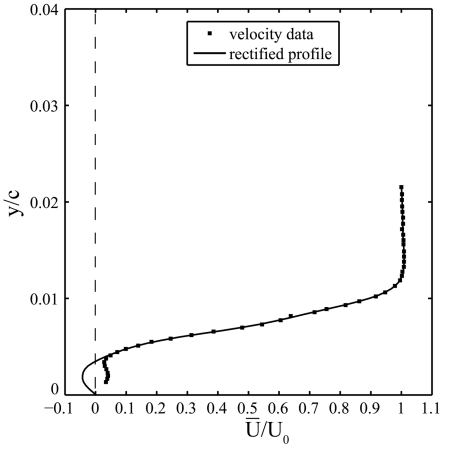

d) Re_c=150×10^3, α=5°, x/c=0.44

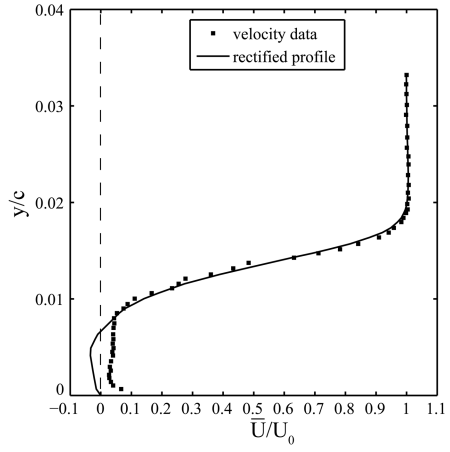

e) Re_c=100×10^3, α=10°, x/c=0.25

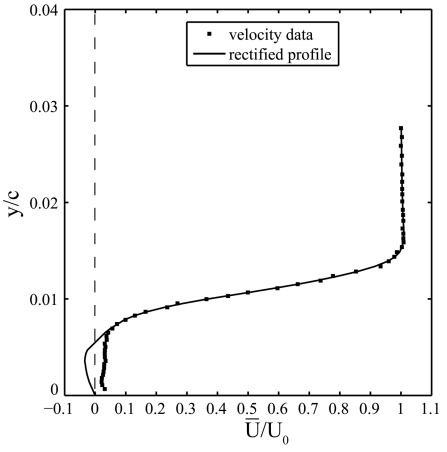

f) Re_c=150×10^3, α=10°, x/c=0.22

Fig. 5 Mean velocity profiles used for stability calculations.

velocity data. In the present study, the numerical solution of Eq. (1) was based on a piecewise-linear approximation of a corrected velocity profile. Specifically, the velocity variation between two adjacent experimental data points is assumed to be linear, providing a simple and reliable method for approximating the velocity profile $\bar{U}(y)$. On each linear interval, Eq. (2) is reduced to

$$\hat{v}'' - \alpha^{*2}\hat{v} = 0 \tag{4}$$

However, to ensure that the pressure and the normal velocity are continuous, the following two matching conditions have to be satisfied at each experimental data point [28]:

$$\Delta\left(\frac{\alpha^*\hat{v}}{\alpha^*\bar{U}-\omega}\right) = 0 \tag{5}$$

$$\Delta\left[(\alpha^*\bar{U}-\omega)\frac{\hat{v}'}{\alpha^*} - \bar{U}'\hat{v}\right] = 0 \tag{6}$$

where $\Delta(\,)$ is the variation of the expression inside the brackets. The dispersion relation given by Eq. (3) was obtained by numerically solving Eq. (4) subject to both the boundary conditions [Eq. (2)] and the matching conditions [Eqs. (5) and (6)]. The numerical procedure was validated using the results of Nishioka et al. [23].

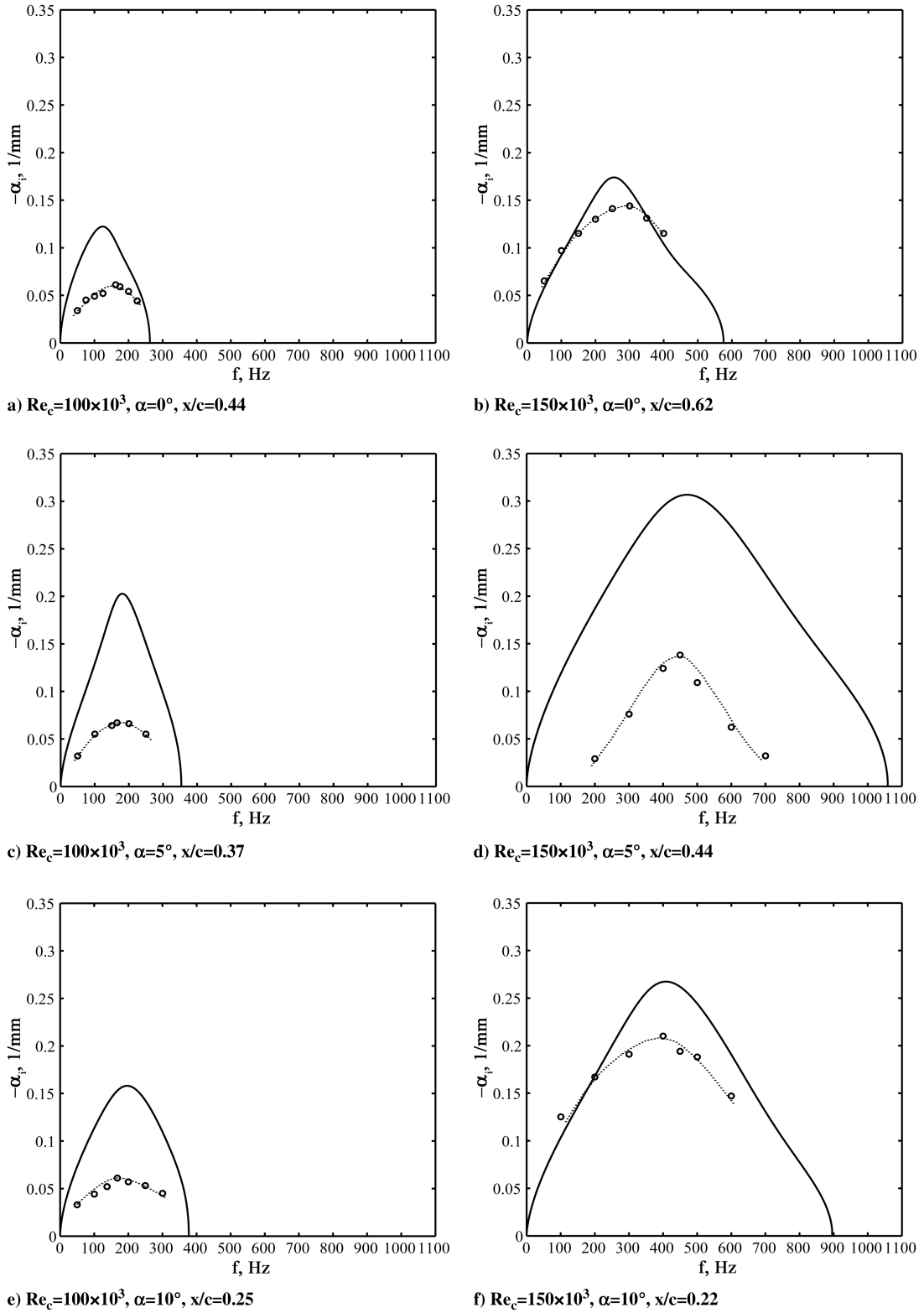

Fig. 6 Disturbance growth rate; solid lines show results of linear stability calculations and symbols show the experimental results.

Figure 6 shows the calculated and experimental growth rates of disturbances ($-\alpha_i$) as a function of frequency ($f = \omega/2\pi$) for $Re_c = 100 \times 10^3$ and 150×10^3. The following procedure was employed to obtain experimental growth-rate velocity data acquired at several streamwise locations. For all of the cases examined, it was verified experimentally that the vertical location corresponding to the maximum amplitude of fluctuations at the fundamental frequency corresponded to that of the maximum rms velocity, agreeing with the results discussed by Dovgal et al. [7]. Thus, at each streamwise location, instantaneous streamwise velocity data acquired at y/c matching the maximum rms velocity were bandpass-filtered. The central frequency of the filter was set to a specific frequency of disturbances for which the growth rate was to be determined and the width of the filter was maintained at 5 Hz, which is sufficiently narrow compared with the overall width of the peaks observed in the velocity spectra (Fig. 4). Root-mean-square values of the filtered signal u'_f were computed at several streamwise locations within the laminar portion of the separated shear layer.

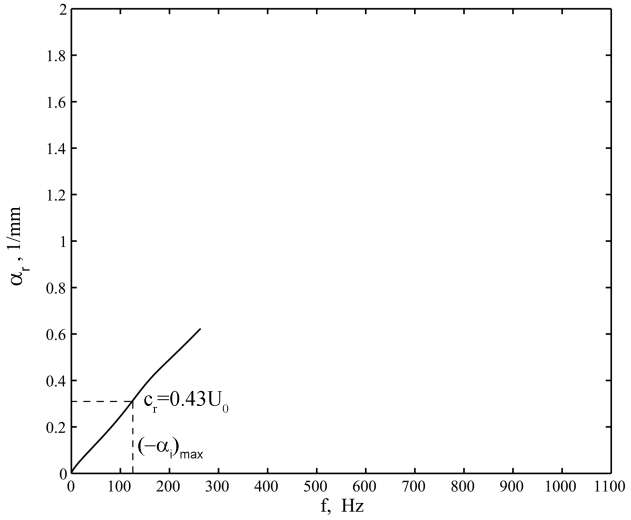

a) Re_c=100×10^3, α=0°, x/c=0.44

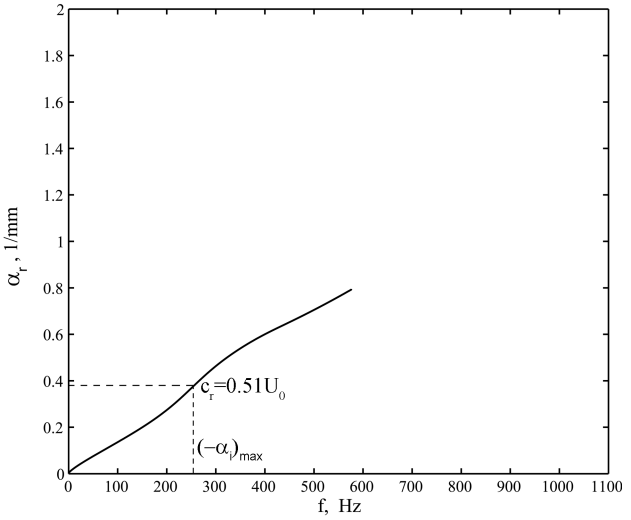

b) Re_c=150×10^3, α=0°, x/c=0.62

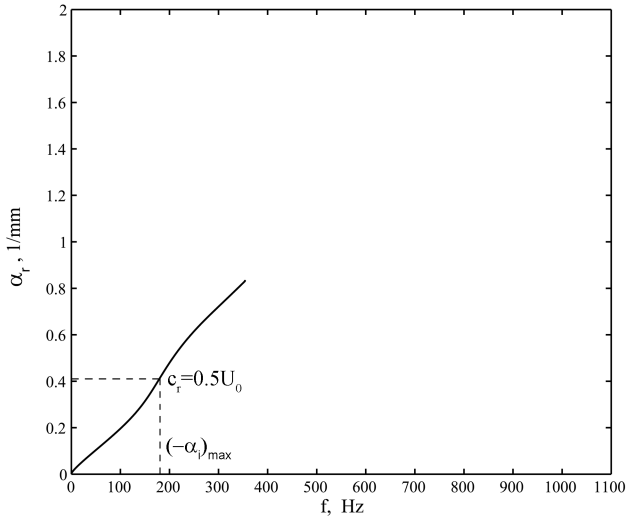

c) Re_c=100×10^3, α=5°, x/c=0.37

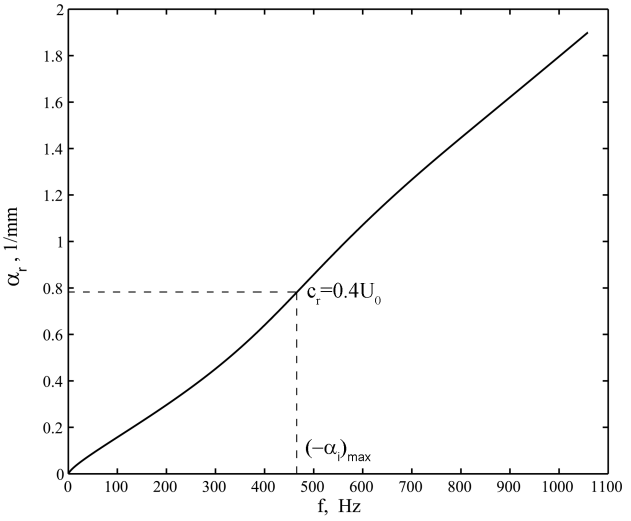

d) Re_c=150×10^3, α=5°, x/c=0.44

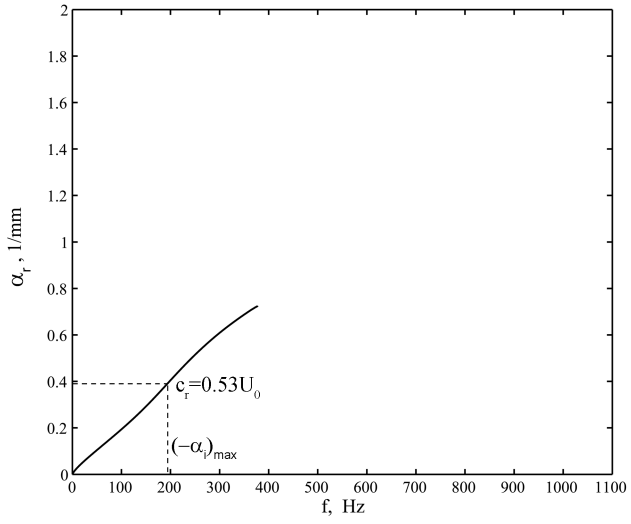

e) Re_c=100×10^3, α=10°, x/c=0.25

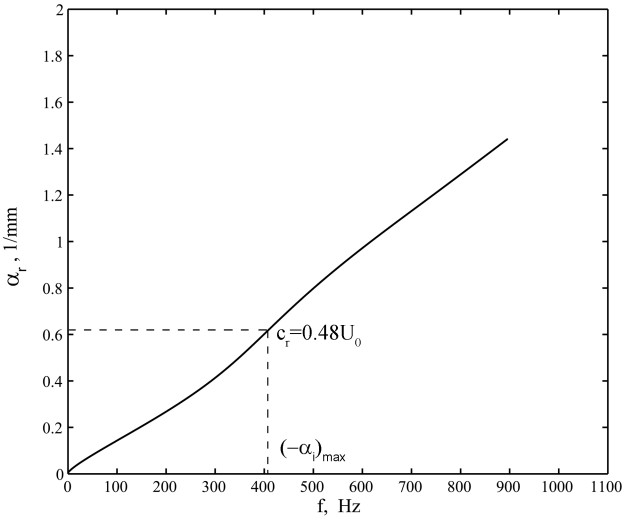

f) Re_c=150×10^3, α=10°, x/c=0.22

Fig. 7 Disturbance wave number from linear stability calculations; dashed lines mark the frequency and the wave number corresponding to the maximum growth rate from Fig. 5; shown values of the propagation speed c_r correspond to the most amplified disturbances.

Because the initial growth of disturbances is nearly exponential, the rate of increase of $\ell n(u'_f)$ with x/c can be used to estimate an average initial growth rate of the disturbances at a given frequency [6,24]. As expected, frequencies associated with the maximum growth rate match the corresponding fundamental frequencies f_0 obtained from the spectral results (Fig. 4). A comparison of the results presented in Fig. 6 shows good agreement between the computed frequencies corresponding to the maximum growth rate of

the disturbances and the corresponding experimental values. For example, for $Re_c = 100 \times 10^3$ at a 5 deg angle of attack, disturbances at $f = 180$ Hz experience the highest growth rate (Fig. 6c). This estimate is approximately 9% higher than the experimental value of $f_0 = 165$ Hz. When the Reynolds number increases to $Re_c = 150 \times 10^3$ at the same angle of attack, the maximum growth rate occurs at $f = 467$ Hz, which is about 2.6% higher than $f_0 = 455$ Hz obtained experimentally.

It should be noted that larger deviations between the fundamental frequencies estimated from stability analysis and those obtained experimentally are observed at a 0 deg angle of attack for both $Re_c = 100 \times 10^3$ and 150×10^3. As noted by Mueller and Batill [14], this may be attributed to increased sensitivity of the flow over symmetrical airfoil profiles at a zero incidence to common experimental uncertainties in setting the angle of attack or the freestream velocity in low Reynolds number flows. In agreement with the observed experimental trends, stability calculations show that an increase of the Reynolds number results in an increase of the growth rate and a widening of the frequency band of amplified disturbances at the corresponding angles of attack. However, the frequency bands of amplified disturbances based on the stability analysis are wider than those based on the experimental data.

The growth rates associated with the most amplified disturbances from inviscid stability calculations are overestimated compared with the corresponding experimental values. A similar trend was observed by Dovgal et al. [7] in data pertaining to a separation bubble forming behind a surface bump. In part, this is to be expected, due to the fact that viscous effects tend to attenuate the growth of natural disturbances in the separated shear layer. However, accounting for viscous effects in [7] did not eliminate the discrepancy between experimental and predicted growth rates, but rather reduced it by about 50%. For more accurate growth-rate estimates, nonparallel effects have to be accounted for [12]. Nevertheless, it can be inferred from the results in Fig. 6 that the frequency-selection process for the most amplified disturbance in the separated shear layer is inviscid in nature.

Figure 7 shows the variation of the disturbance wave number (α_r) with frequency for $Re_c = 100 \times 10^3$ and 150×10^3 obtained from the stability analysis. These results can be used to calculate the propagation speed of the disturbances: $c_r = 2\pi f/\alpha_r$. For example, for $Re_c = 100 \times 10^3$ at $\alpha = 5$ deg, the most amplified disturbance occurs at $f = 180$ Hz (Fig. 6c) and is associated with a wave number of $0.42\ \text{mm}^{-1}$ (Fig. 7c), and so its propagation speed is approximately $0.5U_0$. All computed values of the propagation speed of the most amplified disturbances are shown in the corresponding plots in Fig. 7. These values vary from $0.4U_0$ to $0.53U_0$, agreeing with the results previously reported for separated flows on various geometries [7].

It is of interest to compare the values of c_r with the propagation speed of the roll-up vortices detected in the separated shear layer. This speed can be estimated by means of the fundamental frequency of the shed roll-up vortices (f_0) and the streamwise distance between them (λ): namely, $c_r = \lambda f_0$. These parameters can be obtained from spectral analysis of the hot-wire data (Fig. 4) and from the flow-visualization results (Fig. 2), respectively. For $Re_c = 100 \times 10^3$ at $\alpha = 5$ deg, the outlined approach gives a propagation speed of about $0.55U_0$, which is in good agreement with stability calculations. Also, for $Re_c = 55 \times 10^3$ at $\alpha = 5$ deg, the propagation speed is estimated to be approximately $0.53U_0$.

The comparison of experimental results and stability calculations indicates that the frequency of the most amplified disturbances and their propagation speed can be adequately estimated with inviscid linear stability theory, in agreement with the findings of Nishioka et al. [23] for a flat plate at an incident angle. Consequently, because the roll-up vortices are shed at the frequency matching that of the most amplified disturbance, the roll-up process can be attributed to an inviscid instability. Indeed, the observed roll-up vortices that form as the result of spatially growing disturbances in the separated shear layer are similar in appearance to those produced by the Kelvin–Helmholtz instability in free shear layers.

IV. Conclusions

An experimental investigation and analytical analysis of the separated-shear-layer development on an airfoil model at low Reynolds numbers were carried out. A NACA 0025 airfoil was investigated at three angles of attack: 0, 5, and 10 deg. Detailed experiments were conducted for $Re_c = 100 \times 10^3$ and 150×10^3. At the investigated angles of attack, these two Reynolds numbers are associated, respectively, with the following two flow regimes: 1) flow separation without subsequent reattachment and 2) separation-bubble formation. Spectral analysis of the fluctuating velocity measurements conducted in the separated shear layer suggests that a band of unstable Fourier components is amplified in the separated shear layer. The naturally amplified disturbances are centered at some fundamental frequency. The initial growth at the fundamental frequency is followed by the growth of a subharmonic component, eventually leading to flow transition. The spatial growth of disturbances leads to shear-layer roll-up, and the roll-up vortices are shed at the fundamental frequency. A comparison of stability calculations and experimental results suggests that such important characteristics as the frequency of the most amplified disturbances in the separated shear layer and their propagation speed can be adequately estimated with inviscid linear stability theory. Thus, the shear-layer roll-up on an airfoil, leading to the formation of the roll-up vortices, can be considered to be essentially inviscid in nature. The presented results can be employed for flow control applications, when the fundamental frequency of the naturally growing disturbances needs to be estimated, or to predict salient characteristics of the roll-up vortices.

Acknowledgment

The authors gratefully acknowledge the Natural Sciences and Engineering Research Council of Canada (NSERC) for funding of this work.

References

[1] Carmichael, B. H., "Low Reynolds Number Airfoil Survey," NASA CR-165803, Vol. 1, 1981.

[2] Mueller, T. J., DeLaurier, J. D., "Aerodynamics of Small Vehicles," *Annual Review of Fluid Mechanics*, Vol. 35, 2003, pp. 89–111. doi:10.1146/annurev.fluid.35.101101.161102

[3] Gaster, M., "The Structure and Behaviour of Separation Bubbles," Aeronautical Research Council, Reports and Memoranda No. 3595, London, Mar. 1967.

[4] Horton, H. P., "Laminar Separation in Two and Thee-Dimensional Incompressible Flow," Ph.D. Thesis, Univ. of London, London, 1968.

[5] Watmuff, J. H., "Evolution of a Wave Packet into Vortex Loops in a Laminar Separation Bubble," *Journal of Fluid Mechanics*, Vol. 397, 1999, pp. 119–169. doi:10.1017/S0022112099006138

[6] Boiko, A. V., Grek, G. R., Dovgal, A. V., and Kozlov, V. V., *The Origin of Turbulence in Near Wall Flows*, 1st ed., Springer–Verlag, Berlin, 2002, Chap. 6.

[7] Dovgal, A. V., Kozlov, V. V., and Michalke, A., "Laminar Boundary Layer Separation: Instability and Associated Phenomena," *Progress in Aerospace Sciences*, Vol. 30, No. 1, 1994, pp. 61–94. doi:10.1016/0376-0421(94)90003-5

[8] Haggmark, C. P., Bakchinov, A. A., and Alfredsson, P. H., "Experiments on a Two-Dimensional Laminar Separation Bubble," *Philosophical Transactions of the Royal Society of London, Series A: Mathematical and Physical Sciences*, Vol. 358, 2000, pp. 3193–3205. doi:10.1098/rsta.2000.0704

[9] Marxen, O., Rist, U., and Wagner, S., "Effect of Spanwise-Modulated Disturbances on Transition in a Separated Boundary Layer," *AIAA Journal*, Vol. 42, No. 5, 2004, pp. 937–944. doi:10.2514/1.565

[10] Lang, M., Rist, U., and Wagner, S., "Investigations on Controlled Transition Development in Laminar Separation Bubble by Means of LDA and PIV," *Experiments in Fluids*, Vol. 36, No. 1, 2004, pp. 43–52. doi:10.1007/s00348-003-0625-x

[11] Marxen, O., and Rist, U., "Direct Numerical Simulation of Non-Linear Transitional Stages in an Experimentally Investigated Laminar Separation Bubble," *High Performance Computing in Science and Engineering '05*, edited by W. Nagel, W. Jäger, and M. Resch,

Springer–Verlag, Berlin, 2005, pp. 103–117.
[12] Theofilis, V., Hein, S., and Dallmann, U., "On the Origins of Unsteadiness and Three-Dimensionality in a Laminar Separation Bubble," *Philosophical Transactions of the Royal Society of London, Series A: Mathematical and Physical Sciences*, Vol. 358, 2000, pp. 3229–3246. doi:10.1098/rsta.2000.0706
[13] O'Meara, M. M., and Mueller, T. J., "Laminar Separation Bubble Characteristics on an Airfoil at Low Reynolds Numbers," *AIAA Journal*, Vol. 25, No. 8, 1987, pp. 1033–1041. doi:10.2514/3.9739
[14] Mueller, T. J., and Batill, S. M., "Experimental Studies of Separation on a Two-Dimensional Airfoil at Low Reynolds Numbers," *AIAA Journal*, Vol. 20, No. 4, 1982, pp. 457–464. doi:10.2514/3.51095
[15] Yuan, W., Khalid, M., Windte, J., Scholz, U., and Radespiel, R., "An Investigation of Low-Reynolds-Number Flows Past Airfoils," AIAA Paper 2005-4607, 2005.
[16] Ol, M., McCauliffe, B., Hanff, E., Scholz, U., and Kaehler, C., "Comparison of Laminar Separation Bubble Measurements on a Low Reynolds Number Airfoil in Three Facilities," AIAA Paper 2005-5149, 2005.
[17] Davis, W., Lovato, J., and Pezeshki, C., "Nonlinear Spectral Characterization of Frequency Modulated Control Applied to a Static Airfoil Shear Layer," AIAA Paper 1994-2217, 1994.
[18] Radespiel, R., Windte, J., and Scholz, U., "Numerical and Experimental Flow Analysis of Moving Airfoils with Laminar Separation Bubbles," *AIAA Journal*, Vol. 45, No. 6, 2007, pp. 1346–1356. doi:10.2514/1.25913
[19] Brendel, M., and Mueller, T. J., "Boundary-Layer Measurements on an Airfoil at Low Reynolds Numbers," *Journal of Aircraft*, Vol. 25, No. 7, 1988, pp. 612–617. doi:10.2514/3.45631
[20] Yarusevych, S., Sullivan, P. E., and Kawall, J. G., "Coherent Structures in Airfoil Boundary Layer and Wake at Low Reynolds Numbers," *Physics of Fluids*, Vol. 18, No. 4, 2006, Paper 044101. doi:10.1063/1.2187069
[21] Lin, J. C. M., and Pauley, L. L., "Low-Reynolds-Number Separation on an Airfoil," *AIAA Journal*, Vol. 34, No. 8, 1996, pp. 1570–1577. doi:10.2514/3.13273
[22] Burgmann, S., Brucker, C., and Schroder, W., "Scanning PIV Measurements of a Laminar Separation Bubble," *Experiments in Fluids*, Vol. 41, No. 2, 2006, 319–326. doi:10.1007/s00348-006-0153-6
[23] Nishioka, M., Asai, M., Yoshida, S., "Control of Flow Separation by Acoustic Excitation," *AIAA Journal*, Vol. 28, No. 11, 1990, pp. 1909–1915. doi:10.2514/3.10498
[24] LeBlanc, P., Blackwelder, R., and Liebeck, R., "A Comparison Between Boundary Layer Measurements in a Laminar Separation Bubble Flow and Linear Stability Theory Calculations," *Proceedings of Low Reynolds Numbers Aerodynamic Conference*, edited by T. J. Mueller, Springer–Verlag, Berlin, 1989, pp. 189–205.
[25] Yarusevych, S., "Investigation of Airfoil Boundary Layer and Turbulent Wake Development at Low Reynolds Numbers," Ph.D. Thesis, Univ. of Toronto, Toronto, 2006.
[26] Kawall, J. G., Shokr, M., and Keffer, J. F., "A Digital Technique for the Simultaneous Measurements of Streamwise and Lateral Velocities in Turbulent Flows," *Journal of Fluid Mechanics*, Vol. 133, 1983, pp. 83–112. doi:10.1017/S0022112083001809
[27] Schlichting, H., and Gersten, K., *Boundary Layer Theory*, 8th ed., Springer–Verlag, New York, 2000, Chap. 15.
[28] Drazin, P. G., and Reid, W. H., *Hydrodynamic Stability*, 1st ed., Cambridge Univ. Press, New York, 1981, Chap. 4.
[29] Durst, F., and Zanoun, E. S., "Experimental Investigation of Near-Wall Effects on Hot-Wire Measurements," *Experiments in Fluids*, Vol. 33, No. 1, 2002, pp. 210–218. doi:10.1007/s00348-002-0472-1

F. Coton
Associate Editor